

Synthesis and characterization of Graphene /Nickel nanocomposites: The role of reducing agent on nanoparticle size and morphology

Maryam Salimian*, Gil Goncalves*, Leonard Deepak Francis**, Igor Bdkin*, Marta Ferro***, Catarina Dias****, Joao Ventura**** and Elby Titus*

*Department of Mechanical Engineering / Nanotechnology Research Division (NRD), University of Aveiro, Portugal (m.salimian@ua.pt)

**INL-International Iberian Nanotechnology Laboratory, Braga, Portugal

***Department of Ceramic, University of Aveiro, Portugal

****IFIMUP and IN-Institute of Nanotechnology, and Department of Physics and Astronomy, Faculty of Sciences, University of Porto, Portugal

ABSTRACT

In this work we used one-step approach for the synthesis of reduced graphene oxide (RGO) /Nickel nanocomposites. We also investigated the influence of the reducing agent (hydrazine) on particle size and morphology and the respective influence on magnetic properties. It was shown that magnetic properties are shape anisotropy and dipolar interactions dependence.

Keywords: Graphene oxide, nickel nanoparticles, nanoparticles size and morphology, magnetic properties.

1 INTRODUCTION

Graphene, two dimensional lattice structure of carbon with light weight, flexibility, high surface, and conductivity has got many attention in vast varieties of application like mechanical, optical and electronic disciplines [1]. Functionalization of graphene which modulate its structure and molecular interactions, can effectively influence its final properties in many different applications such as transistors and optoelectronic devices. On the other hand, magnetic particles are of great scientific interest because of their high potential in wide range applications including data storage, magnetic resonance imaging and so on [2,3]. Functionalization of graphene and its related nanostructure with magnetic particles will expand the scope of such properties in the areas which both graphene and magnetic properties are highly desirable like microwave absorption materials [4].

2 EXPERIMENTAL

All chemical reagents were of analytical grade and were used as received. Graphene oxide (GO) was prepared by the chemical exfoliation of graphite (Graphite powder, <45 μm ,

$\geq 99.99\%$, Sigma-Aldrich) following a modified Hummers method [5].

Nickel nitrate $\text{Ni}(\text{NO}_3)_2$ was dissolved in deionized water and was added to the GO solution (1mg/mL) and stirred for two hours. Hydrazine hydrate ($\text{N}_2\text{H}_4 \cdot \text{H}_2\text{O}$) as a reducing agent was added to the solution. The mixture was stirred for one hour and then was transferred to the 25 ml Teflon autoclave and kept in furnace for 22 hours at 100 $^\circ\text{C}$. Resulting solution was washed three times with deionized water and dried by lyophilization.

Four samples were prepared in this way. N_2H_4 concentration was variable while the other conditions were kept constant. RGO/Ni (a), RGO/Ni (b), RGO/Ni (c) and RGO/Ni (d) with hydrazine hydrate concentration of 0.17, 0.81, 1.56 and 4.04 mol/liter respectively.

The synthesized nanocomposites were characterized by XRD, SEM, TEM and VSM.

3 CHARACTERIZATION

Powder X-ray diffraction (XRD) data were collected using Siemens D500 diffractometer with secondary monochromator $\text{CuK}\alpha$ X-radiation in a range from 5 $^\circ$ -80 $^\circ$ with step of 0.05 $^\circ$, the time for collecting x-rays was 50 s for each measuring point at 30 mA and 40 kV.

Morphological studies were performed using an ultra-high resolution analytical scanning electron microscope HR-FESEM Hitachi SU-70 and also with a Quanta 650 FEG ESEM (FEI). Transmission Electron Microscopy (TEM) was performed with a Titan ChemiSTEM 80-200 kV probe Cs corrected microscope.

Magnetic properties study was done with Oxford Instruments Vibrating Sample Magnetometer (VSM), with 40 Hz and 1.5 mm amplitude for the vibration. The measurements were performed at room temperature with parallel magnetic field between 1 and -1T at a rate of 0.3T/min.

4 RESULT AND DISCUSSIONS

It has been reported that oxygen functional groups on the surface of GO can act as a nucleation site for metallic nanoparticles growth. Here, besides of this effect we added N_2H_4 reducing agents in order to control the nickel particles nucleation and growth and its influence on magnetic properties.

XRD analysis represented at Figure 1 can showed the efficiency of the process used on the exfoliation of graphite into graphene oxide. It can be seen that typical strong peak of graphite at 26.6° doesn't appear in GO profile suggesting the complete exfoliation of graphite [6]. XRD pattern of GO has a sharp peak at 10.50° indicating interplanar distance of 0.84 nm caused by the intercalation of oxygen functional groups.

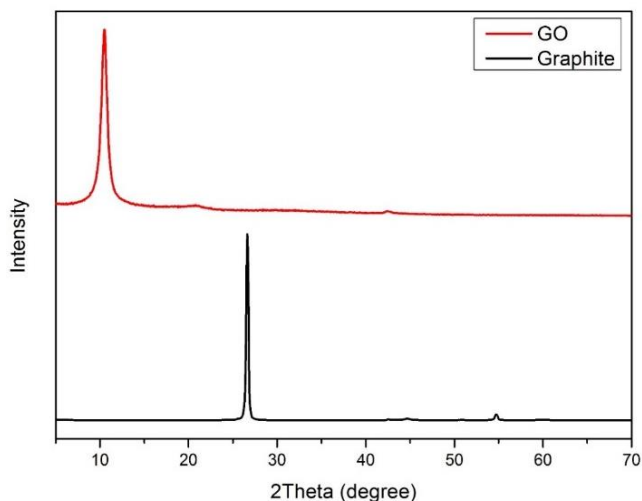


Figure 1: XRD profile pattern of Graphite and synthesized GO

XRD patterns of different RGO/Ni nanocomposites is showed in Figure 2. Diffraction pattern of RGO/Ni (a) which synthesized with the lowest concentration of hydrazine hydrate showed two phases of nickel and nickel hydroxide. Nickel characteristic peaks at 44.7° , 52° and 76.5° are corresponding to (111), (200) and (220) of nickel planes in face-centered cubic structure[7]. The characteristic peaks at 19.38° , 33.32° , 38.78° , 52.13° , 59.38° , 62.98° , 70.23° , corresponding to (001), (100), (101), (102), (110), (111), (200), (103) showed the crystal structure of nickel hydroxide [8] as a second phase in RGO/Ni (a) sample. XRD patterns of RGO/Ni (b), RGO/Ni (c) and RGO/Ni (d) showed only nickel metallic phase in nanocomposite with the same characteristic peaks. The broadened band at around

23° is related to the RGO and it appeared in all XRD pattern.

These data claimed that the crystalline phase obtained on nickel graphene nanocomposites through the hydrothermal reaction of $Ni(NO_3)_2$ varied with the N_2H_4 concentration.

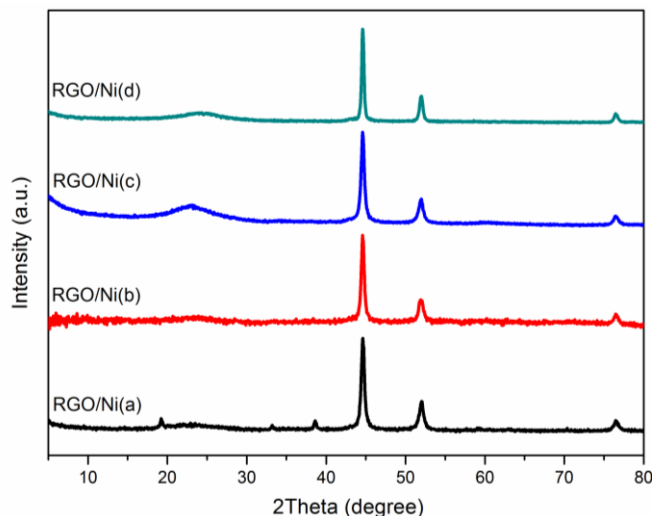


Figure 2: XRD profile pattern of RGO/Ni nanocomposites for different N_2H_4 concentration

SEM images of RGO/Ni nanocomposites represented in Figure 3 and 4 showed that nickel nanoparticles are dispersed and integrated to the surface of RGO sheets. The RGO/Ni (a) nanocomposite showed the formation of spherical nickel particles with the average size of 150 nm, distributed homogeneously on the surface of RGO.

Increasing the N_2H_4 concentration induces drastic changes to the morphology and the size of nickel particles at RGO surface. In this stage spiky nickel particles with the average size of 300 nm RGO/Ni (b) were obtained homogeneously distributed on RGO surface, figure 3.

The sample RGO/Ni (c) showed non-homogenous distribution of nickel particles on the surface of RGO with the particle size of 300 nm. Higher concentration of N_2H_4 on the reaction medium lead to the formation of the nanocomposites with nickel particles agglomerated with the average size of 900 nm on the surface of RGO (RGO/Ni(d)) that can be observed at the Figure 4. These results indicated the crucial role played by N_2H_4 concentration on the control of size and morphology and distribution of nickel particles at RGO/Ni nanocomposites surface.

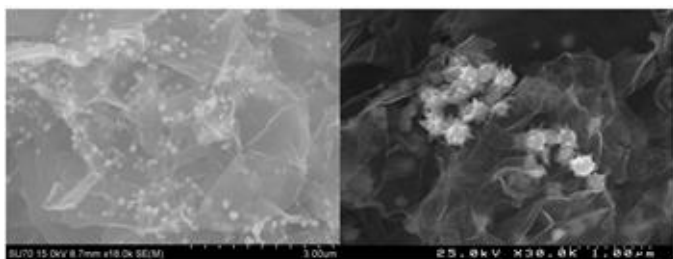


Figure 3: SEM images of RGO/Ni (a) and RGO/Ni (b) left panel and right panel respectively

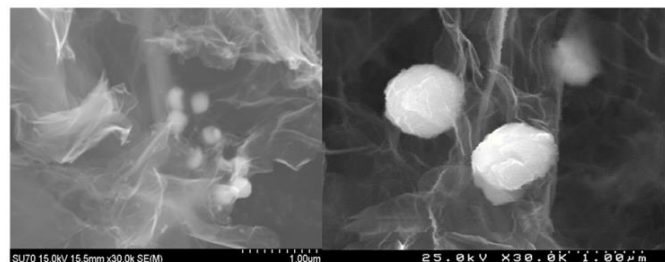


Figure 4: SEM images of RGO/Ni (c) and RGO/Ni (d) left panel and right panel respectively

TEM observation of RGO/Ni(b) was carried for further investigate the spiky morphology of nickel particles (Figure 5). Those nanoparticles are composed by an central nm core of 150 nm surrounded by nanothorns with the size the varies from few nanometer to 100 nm.

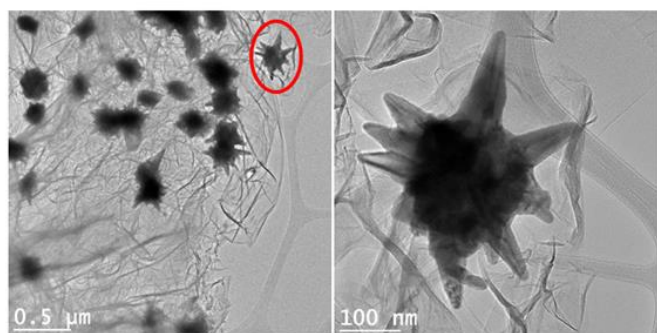


Figure 5: TEM image of RGO/Ni (b) nanocomposite (left panel) and one single spiky nickel nanoparticle on the surface of RGO (right panel).

Magnetic hysteresis (M-H) loops are shown in Figure 6. Related magnetic parameters including saturation magnetization (M_s), remanent magnetization (M_r) and coercivity (H_c) are summarized in table 1. It can be seen that nickel nanoparticles in all samples regardless of their size and morphology exhibited the ferromagnetic behavior. The saturation magnetization (M_s) of all samples are less than

that comparing to bulk nickel due to the surface oxidation. The maximum M_s is 22.8 emu/g belongs to RGO/Ni (a) nanocomposite. For other samples, RGO/Ni (b), RGO/Ni (c) and RGO/Ni (d) magnetic saturation decreasing to 19 emu/g, 14.2 emu/g and 10.4 emu/g respectively. According to the SEM images of sample RGO/Ni (b) and RGO/Ni (c) regarding to nonhomogeneous distribution of nickel particles it can be concluded that the density of nickel particles for two tested samples are different from each other and also are lower than RGO/Ni (a) and RGO/Ni (b). However the effective magnetization of nickel should be determined by establishment of nickel percentage in each nanocomposite. M_s for RGO/Ni (a) is higher than RGO/Ni (b). As both samples showed the homogeneous distribution on RGO sheets. This difference can be arisen from the fact that the spiky nickel nanoparticles in RGO/Ni (b) nanocomposite have higher surface area than those spherical particles in RGO/Ni (a) nanocomposite. All samples exhibited higher values of coercivity comparing to the bulk nickel value. Coercivity of three nanocomposites RGO/Ni (a), RGO/Ni (c) and RGO/Ni (d) are 146, 147 and 165 Oe which showed by increasing the particle size the coercivity values were increased.

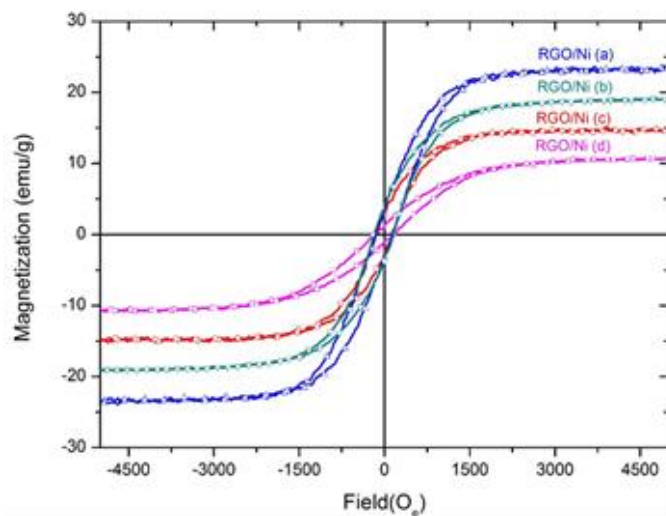


Figure 6: Magnetic hysteresis (M-H) loops of RGO/Ni nanocomposite samples at room temperature.

RGO/Ni(b) with nickel spiky morphology showed the highest coercivity value of 182 Oe, this value for bulk nickel is around 0.7 Oe. This result can be attributed to the shape anisotropy of nickel particles [9-11].

Sample	M _s	Mr	Hc
	emu/g	emu/g	Oe
RGO/Ni(a)	22.8	3.3	146
RGO/Ni(b)	19	3.5	182
RGO/Ni(c)	14.2	2.6	147
RGO/Ni(d)	10.4	1.1	165

Table 1: magnetic parameters of RGO/Ni nanocomposites

5 CONCLUSION

The hydrothermal method used for synthesis of reduced graphene oxide/nickel nanocomposites allows to control the size and morphology of nickel nanoparticles and simultaneously reduce the graphene oxide surface. It was shown that hydrazine hydrate acts as a reducing agent and has a fundamental role on the control of the size and morphology of nickel particles. Magnetic properties study claimed the ferromagnetic characteristic of all nanocomposites. Saturation magnetization of all samples are less than that of bulk material, likely related to the surface oxidation. RGO/Ni (b) showed the highest coercivity among all the samples and higher than that of bulk nickel due to the spiky shape of nickel particles and dipolar interactions.

REFERENCES

- [1] Matthew J. Allen, Vincent C. Tung, and Richard B. Kaner, *Chem. Rev.*, 110, 132–145, 2010
- [2] Li, Z., Wei, L., Gao, M. Y. and Lei, H., *Adv. Mater.*, 17, 1001–1005, 2005
- [3] Taeghwan Hyeon, *Chem. Commun.*, 927-934, 2003
- [4] Xiaoxia Wang, Mingxun Yu, Wei Zhang, Baoqin Zhang, Lifeng Dong, *Appl. Phys. A* 118:1053–1058, 2015
- [5] Gil Goncalves, Paula A. A. P. Marques, Carlos M. Grandeiro, Helena I. S. Nogueira, M. K. Singh, and J. Gracio, *Chem. Mater.*, 21, 4796–4802, 2009
- [6] Luyang Wang, Younghun Park, Peng Cui, Sora Bak, Hanleem Lee, Sae Mi Lee and Hyoyoung Lee, *Chem. Commun.*, 50, 1224-1226, 2014
- [7] Guo-Xing Zhu, Xian-Wen Wei and Shan Jiang, *J. Mater. Chem.*, 17, 2301-2306, 2007
- [8] Jianjun Wang, Huan Pang, Jingzhou Yin, Lina Guan,

Qingyi Lu and Feng Gao *CrystEngComm*, 12, 1404-1409, 2010

- [9] Zhongli Li, Yanjie Su, Yijian Liu, Jian Wang, Huijuan Geng, Poonam Sharma and Yafei Zhang, *CrystEngComm*, 16, 8442-8448, 2014.
- [10] Ambily Mathew, N. Munichandraiah, G. Mohan Rao, *Materials Science and Engineering: B*, 158, 7-12, 2009
- [11] Zhenyuan Ji, Xiaoping Shen, Guoxing Zhu, Hu Zhou and Aihua Yuan, *J. Mater. Chem.*, 22, 3471-3477, 2012